CHIN. PHYS. LETT. Vol. 27, No. 10 (2010) 104702

Singular Wave Solutions of Two Integrable Generalized KdV Equations *

ZHANG Zheng-Di(张正娣), BI Qin-Sheng(毕勤胜)**
Faculty of Science, Jiangsu University, Zhenjiang 212013

(Received 25 March 2010)

We present some singular wave solutions such as multi-peaked periodic waves, multi-peaked kink waves, multi-peaked peakons as well as kink-compactons, associated with singular curves of generalized KdV equation and modified KdV equation. When a trajectory intersects with the singular curve, it may be divided into segments. Different combinations of these segments may lead to different singular wave solutions, while at the intersection points, peaks on the waves can be observed.

PACS: 47. 35. +i, 05. 45. Yv, 11. 10. Ef, 11. 10. Lm DOI: 10.1088/0256-307X/27/10/104702

Solitons were first introduced as solutions of unidirectional nonlinear wave equations, obtained via asymptotic expansions around simple wave motion of Euler equations for shallow water.[1] Later developments identified some of these water wave equations as completely integrable Hamiltonian systems solvable by inverse scattering transform (IST) method.[2] The integrability of such bi-Hamiltonian systems is a consequence of the following general results proven independently in Refs. [3,4]. Assuming that, for all values of the constant parameter λ, the operator $\theta_1 + \lambda\theta_2$ is Hamiltonian, then each member of the hierarchy equations $q_t = \sum_{j=1}^{N} c_j(\theta_2\theta_1^{-1})^j q_x$ ($N \in$ Z, c_j constant) is an integrable equation in the sense that it is a bi-Hamiltonian system possessing infinitely many conserved quantities.[5] Defining $\theta_2 = \partial_x + \beta\partial_x^3 + \frac{1}{3}\alpha(q\partial_x + \partial_x q)$, then $q_t + (\theta_2\theta_1^{-1})q_x = 0$ yields the KdV equation for $\theta_1 = \partial_x$, $q = u$, while for $\theta_1 = \partial_x + \nu\partial_x^3$ and $q = u + u_x$, it leads to a generalized KdV equation expressed as

$$u_t + u_x + \nu u_{xxt} + \beta u_{xxx} + \alpha u u_x + \frac{1}{3}\alpha\nu(u u_{xxx} + 2u_x u_{xx}) = 0. \quad (1)$$

Furthermore, the operator $\theta_2 = \partial_x + \beta\partial_x^3 + 2(\frac{1}{3}\alpha q + \mu\alpha^2 q^2)\partial_x + q_x\partial_x^{-1}(\frac{1}{3}\alpha + 2\mu\alpha^2 q)\partial_x$, together with $\theta_1 = \partial_x + \nu\partial_x^3$, $q = u + \nu u_{xx}$ and $q_t + (\theta_2\theta_1^{-1})q_x = 0$, yields the following modified KdV equation:

$$\begin{aligned} &u_t + u_x + \nu u_{xxt} + \beta u_{xxx} + \alpha u u_x \\ &+ \frac{1}{3}\nu\alpha(u u_{xxx} + 2u_x u_{xx}) + 3\mu\alpha^2 u^2 u_x \\ &+ \nu\mu\alpha^2(u^2 u_{xxx} + u_x^3 + 4u u_x u_{xxx}) \\ &+ \nu^2\mu\alpha^2(u_x^2 u_{xxx} + 2u_x u_{xx}^2) = 0. \end{aligned} \quad (2)$$

Equations (1) and (2) can also be derived by employing the modeling of water waves as well as general asymptotic considerations.

In a particular Galilean frame, the singular curves, which was first presented from a physical model,[6,7] may be observed evolving the complexity of the solutions. The importance of such singular curves is that it can cause appearance of a variety of singular wave patterns including peakons and compactons.[8–10]

In this Letter, we report two main results. First, we identify how the singular curves influence the phase portraits of the two topological vector fields. Transition boundaries on which bifurcations may occur can then be defined to divide the parameter space into different regions associated with different types of waves. Second, we present some new wave patterns as well as new behaviors. As we know, each trajectory on the phase plane may correspond to one possible solution of the systems, while it is not true if the trajectory meets with the singular curves, for the fact it may be divided into segments by the singular curves. Different combinations of these segments may lead to different wave patterns. Peaks can be observed at the intersection point. Specially, new waves such as multi-peaked periodic waves, multi-peaked kink-waves, kink-compactons can be obtained.

Moving (1) into the particular Galilean frame and integrating the resultant equations yields a planar Hamiltonian vector field by defining $y = u_\xi$ for traveling wave $u = u(x - ct) = u(\xi)$, with a vertical singular line $(\beta - c\nu) + \frac{1}{3}\alpha\nu u = 0$. For avoiding the singular line temporarily we take the transformation $d\xi = [(\beta - c\nu) + \frac{1}{3}\alpha\nu u]d\tau$, then (1) becomes a planar Hamiltonian vector field with the first integral $H = gu + \frac{1}{2}(1-c)u^2 + \frac{1}{2}(\beta - c\nu)y^2 + \frac{1}{6}\alpha u^3 + \frac{1}{6}\alpha\nu u y^2$, where g is an integral constant. The possible equilibrium points can be written as $u_{e\pm} = \frac{1}{\alpha}[-(1-c) \pm \sqrt{(1-c)^2 - 2\alpha g_1}]$, $y_e = 0$, while the singular curve give rise to two equilibrium points: $u_s = -\frac{3}{\alpha\nu}(\beta - c\nu)$, $y_{s\pm} = \pm\sqrt{-\frac{6}{\alpha\nu}f(u_s)}$. The properties of these equilibrium points can be determined by eigenvalues of the linearlized matrix associated. Assuming $(1-c)^2 - 2\alpha g_1 > 0$, we can define the following two transition boundaries, $u_s = u_{e\pm}$, on which bifurcation phenomena can be observed. The transition boundaries divide the parameter space into different regions associated with the following five typical phase portraits plotted in Fig. 1 (SL represents the singular line).

Two types of Peaked periodic waves can be found

*Supported by the National Natural Science Foundation of China under Grant Nos 10872080 and 10972091.
**Email: qbi@ujs.edu.cn
© 2010 Chinese Physical Society and IOP Publishing Ltd

for the conditions $u_{e-} < u_s < u_{e+}$, $H = H(u_s, 0)$, which can be expressed as

$$\pm(\xi - \xi_0) = \sqrt{\nu}\big[\pi - 2\sin^{-1}(\sqrt{U_1 - u}/\sqrt{U_1 - U_2})\big] + nT_1,\ \xi \le T_1/2,\ u \in [U_2, u_s], \tag{3}$$

associated with the path $H_2^{(1)}$ with the period $T_1 = 2\sqrt{\nu}\{\pi - 2\sin^{-1}[\sqrt{(U_1 - u_s)/(U_1 - U_2)}\}$, while for $H_2^{(2)}$

$$\pm(\xi - \xi_0) = -2\sqrt{\nu}\sin^{-1}(\sqrt{U_1 - u}/\sqrt{U_1 - U_2}) + nT_2,\ \xi \le T_2/2,\ u \in [u_s, U_1], \tag{4}$$

where $T_2 = 4\sqrt{\nu}\sin^{-1}[\sqrt{(U_1 - u_s)/(U_1 - U_2)}]$, ξ_0 is the constant phase at which $u = U_{2,1}$and peaks can be observed at $\xi = \xi_0 \pm \frac{1}{2}nT_{1,2}$, respectively, $U_{1,2} = [-3(\nu - \beta) \pm \sqrt{9\nu^2 + 18\nu\beta - 27\beta^2 - 36c\nu^2 - 36c\nu\beta - 24g\alpha\nu^2}$ represent the intersection coordinates between the trajectory and u-axis.

Kink-compactons can be observed for the conditions $H_0 = H(u_{e-}, 0)$, $u_s < u_{e-}$, or $H_0 = H(u_{e+}, 0)$, $u_s > u_{e+}$. Homoclinic orbits $H_1^{(3)}$ and $H_3^{(3)}$ can be found, which form solitions. However, the trajectories $H_1^{(1)}$, $H_1^{(2)}$, $H_3^{(1)}$ and $H_3^{(2)}$ correspond to a new type of wave patterns, which is called the kink-compactons here, combining both half structures of kink waves and compactons. We only present the expressions of the new wave associated with $H_1^{(1)}$ (implying $H(u, 0) = \frac{1}{6}\alpha(u - u_{e-})^2(u - u_{e2})$) for $u \in [u_s, u_{e-}]$, written in the form

$$\begin{aligned}
&\xi_0 - \xi = R_1 + 2\sqrt{\nu}\tan^{-1}\left(\sqrt{\frac{u - u_s}{u_{e2} - u}}\right) - \sqrt{\nu}\sqrt{\frac{u_{e-} - u_s}{u_{e2} - u_{e-}}}\ln\frac{1 + \sqrt{(u_{e2} - u_{e-})(u - u_s)/(u_{e-} - u_s)(u_{e2} - u)}}{1 - \sqrt{(u_{e2} - u_{e-})(u - u_s)/(u_{e-} - u_s)(u_{e2} - u)}},\\
&\qquad u_s < u < u_0,\\
&\xi - \xi_0 = -2\sqrt{\nu}\tan^{-1}\left(\sqrt{\frac{u - u_s}{u_{e2} - u}}\right) + \sqrt{\nu}\sqrt{\frac{u_{e-} - u_s}{u_{e2} - u_{e-}}}\ln\frac{1 + \sqrt{(u_{e2} - u_{e-})(u - u_s)/(u_{e-} - u_s)(u_{e2} - u)}}{1 - \sqrt{(u_{e2} - u_{e-})(u - u_s)/(u_{e-} - u_s)(u_{e2} - u)}} - R_1,\\
&\qquad u_0 < u \le u_{e-},
\end{aligned} \tag{5}$$

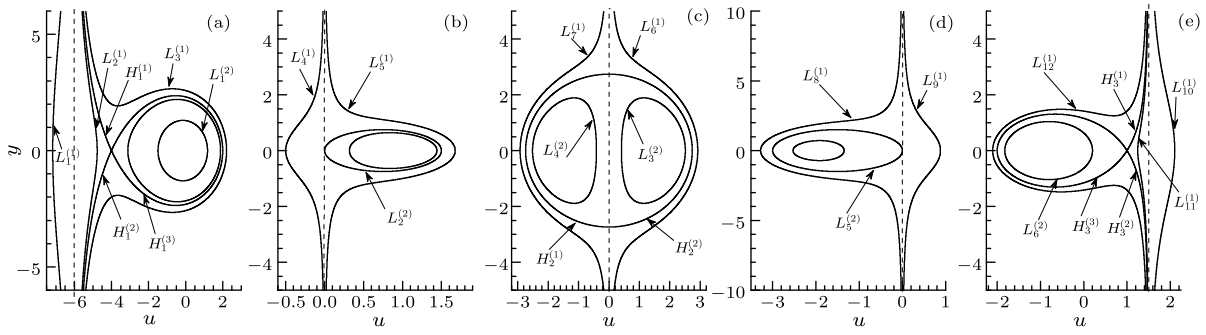

Fig. 1. Typical phase portraits for (a) $u_s < u_{e-}$, (b) $u_s = u_{e-}$ (c) $u_{e-} < u_s < u_{e+}$, (d) $u_s = u_{e+}$ (e) $u_s > u_{e+}$. The trajectories, $L_i^{(1)}$, $i = 1, \cdots, 12$ correspond to compactons, the trajectories, $L_i^{(2)}$, $i = 1, \cdots, 6$ correspond to smooth periodic waves, while the dot line corresponds to the singular line.

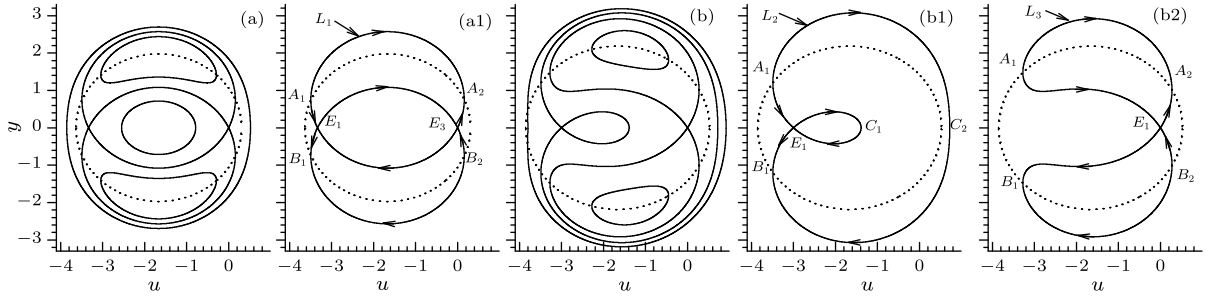

Fig. 2. Typical phase portraits on the total phase plane. The dotted line corresponds to the singular line. (a) For the parameters fixed at $g = 0$, $\mu = \frac{1}{10}$, $\nu = 1$, $\alpha = 1$, $c = \frac{4}{9}$, $\beta = \frac{1}{3}$. The corresponding Hamiltonian values at the five equilibrium points are $H_1(-\frac{10}{3}, 0) = H_3(0, 0) = 0$, $H_2(-\frac{5}{3}, 0) = \frac{125}{648}$, $H_{4,5}(-\frac{15}{11}, \frac{9\sqrt{7}}{11}) = -\frac{5}{27}$. Two intersection points between the singular curve and the axis $y = 0$ can be observed. L_1 is the trajectory related to the condition $H(u, y) = 0$. (b) For the parameters fixed at $g = 0$, $\mu = \frac{1}{10}$, $\nu = 1$, $\alpha = 1$, $c = \frac{2}{5}$, $\beta = \frac{1}{5}$. The corresponding Hamiltonian values at the five equilibrium points are $H_1(-3, 0) = 0.225$, $H_2(-2, 0) = 0.267$, $H_3(0, 0) = 0$, $H_{4,5}(-\frac{15}{11}, \frac{9\sqrt{7}}{11}) = -0.3273$. Two intersection points between the singular curve and the axis $y = 0$ can be observed. L_2 is the trajectory for $H(u, y) = H_1(-3, 0)$, while L_3 is for $H(u, y) = 0$

where ξ_0 represents the constant phase at which $u = u_0$ $(u_s < u_0 < u_{e-})$,

$$R_1 = -2\sqrt{\nu}\tan^{-1}\left(\sqrt{\frac{u_0-u_s}{u_{e2}-u_0}}\right) + \sqrt{\frac{\nu(u_{e-}-u_s)}{u_{e2}-u_{e-}}} \cdot \ln\frac{1+\sqrt{(u_{e2}-u_{e-})(u_0-u_s)/(u_{e-}-u_s)(u_{e2}-u_0)}}{1-\sqrt{(u_{e2}-u_{e-})(u_0-u_s)/(u_{e-}-u_s)(u_{e2}-u_0)}}. \quad (6)$$

Remark: For the upper path $H_1^{(1)}$, if $u \to u_s$, from the expressions (5), one may find $\xi = \xi_0 - R_1 < -\infty$; for $u \to u_{e-}$, we have $\xi \to +\infty$, which implies the wave combines both half structures of compacton and kink wave.

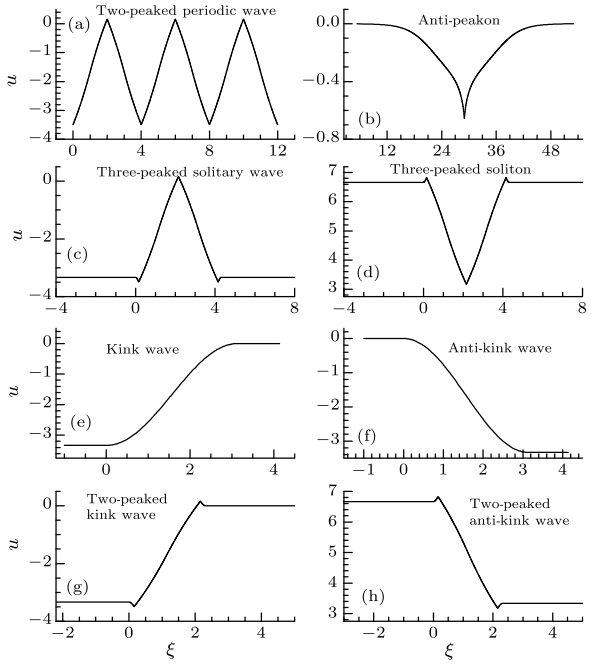

Fig. 3. Different types of wave solutions in Fig. 2(a1) for the trajectory moving as (a) $A_1 \to A_2 \overset{\text{jump}}{\longrightarrow} B_2 \to B_1 \overset{\text{jump}}{\longrightarrow} A_1$; (b) $E_1 \to B_1 \overset{\text{jump}}{\longrightarrow} A_1 \to E_1$; (c) $E_1 \to B_1 \overset{\text{jump}}{\longrightarrow} A_1 \to A_2 \overset{\text{jump}}{\longrightarrow} B_2 \to B_1 \overset{\text{jump}}{\longrightarrow} A_1 \to E_1$; (d) $E_3 \to A_2 \overset{\text{jump}}{\longrightarrow} B_2 \to B_1 \overset{\text{jump}}{\longrightarrow} A_1 \to A_2 \overset{\text{jump}}{\longrightarrow} B_2 \to E_3$; (e) $E_1 \to E_3$; (f) $E_3 \to E_1$; (g) $E_1 \to B_1 \overset{\text{jump}}{\longrightarrow} A_1 \to A_2 \overset{\text{jump}}{\longrightarrow} B_2 \to E_3$; (h) $E_3 \to A_2 \overset{\text{jump}}{\longrightarrow} B_2 \to B_1 \overset{\text{jump}}{\longrightarrow} A_1 \to E_1$.

A similar procedure can be employed for the modified KdV equation (2). A quadratic singular curve, $(\beta - c\nu) + \frac{1}{3}\alpha\nu u + \nu\mu\alpha^2 u^2 + \mu\nu^2\alpha^2 y^2 = 0$, can be found evolving the topological vector field.[11] By defining $d\xi = [(\beta - c\nu) + \frac{1}{3}\alpha\nu u + \nu\mu\alpha^2 u^2 + \alpha\mu\nu^2\alpha^2 y^2]d\eta$, the system (2) can be written as a planar vector field with the first integral $H(u,y) = \frac{1}{2}[2gu + (1-c)u^2 + (\beta - c\nu)y^2] + \frac{1}{6}\nu\alpha u y^2 + \frac{1}{6}\alpha u^3 + \frac{1}{4}\mu\alpha^2(u^2+\nu y^2)^2$. The equilibrium points can be obtained as $u_1 = 0$, $u_{2,3} = -\frac{1}{4\mu\alpha}[1 \pm \sqrt{\Delta}]$, where $\Delta = 1 + 16(c-1)\mu$. In addition, two equilibrium points, denoted by $u_s = \frac{3(\beta - c\nu)}{\alpha[18\mu(\nu-\beta)-\nu]}$, $y_{s\pm} = \pm\sqrt{-[(\beta - c\nu) + \frac{1}{3}\alpha\nu u_s + \nu\mu\alpha^2 u_s^2]/\mu\nu^2\alpha^2}$, can be found associated with the singular curve. Detailed bifurcation analysis has revealed different phase portraits associated with the parameters.[12] Here we only focus on the trajectories associated novel wave patterns in three typical types of phase portraits, which are plotted in Fig. 2.

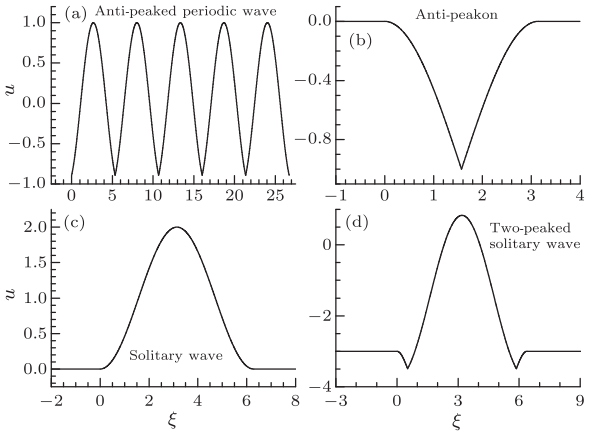

Fig. 4. Different wave solutions in Fig. 2(b1) for the trajectory moving as (a) $A_1 \to C_2 \to B_1 \overset{\text{jump}}{\longrightarrow} A_1$; (b) $E_1 \to B_1 \overset{\text{jump}}{\longrightarrow} A_1 \to E_1$; (c) $E_1 \to C_1 \to E_1$; (d) $E_1 \to B_1 \overset{\text{jump}}{\longrightarrow} A_1 \to C_2 \to B_1 \overset{\text{jump}}{\longrightarrow} A_1 \to E_1$.

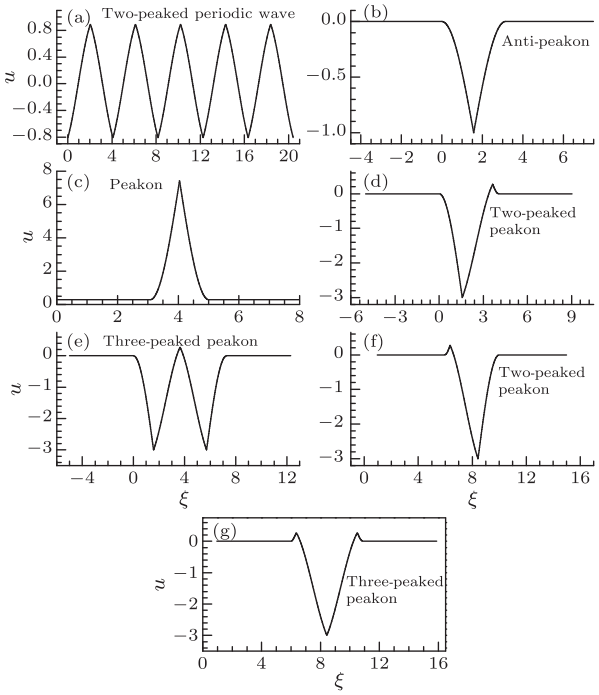

Fig. 5. Different types of wave solutions in Fig. 2(b2) for the trajectory moveing as (a) $A_1 \to A_2 \overset{\text{jump}}{\longrightarrow} B_2 \to B_1 \overset{\text{jump}}{\longrightarrow} A_1$; (b) $E_1 \to B_1 \overset{\text{jump}}{\longrightarrow} A_1 \to E_1$; (c) $E_1 \to A_2 \overset{\text{jump}}{\longrightarrow} B_2 \to E_1$; (d) $E_1 \to B_1 \overset{\text{jump}}{\longrightarrow} A_1 \to A_2 \overset{\text{jump}}{\longrightarrow} B_2 \to E_1$; (e) $E_1 \to B_1 \overset{\text{jump}}{\longrightarrow} A_1 \to A_2 \overset{\text{jump}}{\longrightarrow} B_2 \to B_1 \overset{\text{jump}}{\longrightarrow} A_1 \to E_1$; (f) $E_1 \to A_2 \overset{\text{jump}}{\longrightarrow} B_2 \to B_1 \overset{\text{jump}}{\longrightarrow} A_1 \to E_1$; (g) $E_1 \to A_2 \overset{\text{jump}}{\longrightarrow} B_2 \to B_1 \overset{\text{jump}}{\longrightarrow} A_1 \to A_2 \overset{\text{jump}}{\longrightarrow} B_2 \to E_1$.

Generally, each trajectory on the phase plane corresponds to a possible solution.[13] However, for these typical trajectories L_1, L_2, L_3, which intersect with the singular curves, $u_{\xi\xi}$ does not exist at these intersection points, implying non-smooth phenomena occur.[14] Two different directions on each intersection point can be observed. With the variations of ξ, the trajectories, moving at the intersection points, no longer passing across the intersection points along the original orbits, may jump between the intersection points A_1 and B_1 or A_2 and B_2, which forms peaks. These trajectories are divided into segments by the singular curve, while different combinations of these segments form different types of singular waves, among which typical wave patterns can be observed. The details of the typical wave forms related to the trajectories L_1, L_2, L_3 have been presented in Figs. 3–5 by numerical simulation.

For trajectory not intersecting with the singular curve, a regular wave solution can be integrated numerically, as we have expected. However, when a trajectory intersects with the singular curve, it may be divided into segments by the singular curve. Different combinations of these segments may lead to different types of singular curves. Trajectories may jump between the intersection points to form peaks on the wave, which leads the smooth wave solutions to non-smooth solutions. This study confirms that the structures of peaked-periodic waves, peakons, antipeakons, compactons, kink waves and anti-kink waves can be combined together to form more general solitons. Different wave solutions may coexist corresponding to the namely same phase trajectories intersecting with the singular curves according to the special evolutions of the trajectories with the variation of the variable ξ. More complex structures of the wave solutions can be further derived by assuming different combination of the segments of the trajectories. For example, the wave solution associated with the trajectory $E_1 \to A_2 \overset{\text{jump}}{\longrightarrow} B_2 \to B_1 \overset{\text{jump}}{\longrightarrow} A_1 \to A_2 \overset{\text{jump}}{\longrightarrow} B_2 \to B_1 \overset{\text{jump}}{\longrightarrow} A_1 \to A_2 \overset{\text{jump}}{\longrightarrow} B_2 \to E_1$, for L_3, since at each intersection point, there always exist two possible choices for the direction of the trajectory process.

References

[1] Whitham G B 1974 *Linear and Nonlinear Waves* (New York: Wiley Interscience)
[2] Johnson R S 1979 *Phys. Lett.* A **72** 197
[3] Gel'fand I M and Dorfman I 1979 *Funct. Anal. Appl.* **13** 248
[4] Fokas A S and Fuchssteiner B 1980 *Lett. Nuovo Cimento* **28** 299
[5] Fokas A S 1995 *Physica* D **87** 145
[6] Dai H H 1998 *Wave Motion* **28** 367
[7] Bi Q S 2005 *Phys. Lett.* A **344** 361
[8] Dullin H R, Gottwald G A and Holm D D 2001 *Phys. Rev. Lett.* **87** 1772
[9] Li J and Zhang J 2004 *Chaos, Solitons and Fractals* **21** 899
[10] Dai H H and Huo Y 2000 *Proc. Roy. Soc. London* A **456** 331
[11] Bi Q S and Zhang Z D 2008 *Phys Rev.* E **77** 036607
[12] Camassa R and Holm D D 1993 *Phys. Rev. Lett.* **71** 1661
[13] Zhang Z D and Bi Q S 2008 *Phys. Lett.* A **372** 3243
[14] Zhang Z D and Bi Q S 2009 *Chin. Phys. Lett.* **26** 010503